Supplementary Information for

ATP-fuelled self-assembly to regulate chemical reactivity in the time domain

Maria A. Cardona, Leonard J. Prins*

Department of Chemical Sciences, University of Padova, Via Marzolo 1, 35131 Padova, Italy.

Table of Contents

1. Materials and methods

1.1 Instrumentation

NMR Analysis: ^{1}H were recorded using a Bruker spectrometer operating at 300 MHz for ^{1}H. ^{13}C NMR (proton decoupled) were recorded on a Bruker AV500 operating at 500 MHz for ^{1}H and at 126 MHz for ^{13}C. Chemical shifts, δ are reported in ppm and were referenced against TMS (δ_H = 0.00 ppm) or the solvent residual peak (δ_H = 7.26 for $CDCl_3$, δ_H = 2.49 ppm for DMSO-$d_5$residual peak, δ_H = 3.31 for CD_3OD residual peak), (δ_C = 77.16 ppm for $CDCl_3$, δ_C = 39.52 ppm for DMSO-$d_5$residual peak, δ_C = 49.00 for CD_3OD residual peak).[1]Abbreviations for multiplicity are as follows: s = singlet, br s = broad singlet, d = doublet, t = triplet, q = quartet, m = multiplet, dd = doublet of doublet, etc.).

MS Measurements: ESI-MS measurements were acquired on an Agilent Technologies 1100 Series LC/MSD Trap-SL spectrometer, equipped with an ESI source, hexapole filter and ionic trap.

pH Measurements: The pH of buffer solutions was determined at room temperature using a Metrohm-632 pH meter equipped with a Ag/AgCl/KCl reference electrode and calibrated with standard buffer solutions at pH 7.00 and pH 10.00.

UV-Vis Measurements: UV-Vis measurements were recorded on a Varian Cary50 spectrophotometer holding a thermostatted multiple cuvette holder or a Varian Cary100 spectrophotometer hosted with a thermostatted multiple cuvette holder. Individual spectra were acquired in Scan Mode while kinetics were followed in Scanning Kinetics Mode. The spectra were then exported and analysed using Excel and plotted using Origin. Analysis were conducted using 1 mL Quartz cuvettes.

Fluorescence Spectroscopy: Fluorescence measurements were recorded on a Varian Cary Eclipse fluorescence spectrophotometer equipped with a thermostated cell holder hosting a maximum of 4 cuvettes. Experiments were typically conducted in 1 mL fluorescence quartz cuvettes. Fluorescence spectra were obtained in either scan mode orkinetics mode in which the emission at a particular wavelength was monitored over time. After each addition of the respective component to the sample cuvette, the sample was allowed to equilibrate before measurement.

HPLC Analysis: The HPLC analysis were performed on an Agilent Technologies 1290 Infinity equipped with a DAD detector and a Quadrupole LC/MS.Conditions: Flow rate: 0.6 ml/min, Gradient: 5-95%B (A: H_2O+0.1%HCOOH, B: ACN+ 0.1% HCOOH) from 0.00 to

5.00 min; 95-100 % B in 5 to 5.10 min; 100 % B from 5.10 to 8.10 min; 100-5 % B in 8.10 to 9.10 min; and finally 5% B from 9.10 to 10.00 min. Column: Agilent Zorbax SB-C3 Rapid Resolution HT 3.0 × 100 mm 1.8 micron. Injection volume: 20 µL Column temperature: 40 ^{o}C.

DLS Analysis: DLS measurements were recorded on a Malvern Zetasizer Nano-S instrument. Samples were analysed in disposable low volume cuvettes.

TEM Analysis: TEM images were recorded on a Jeol 300 PX electron microscope. One drop of sample was placed on the sample grid for 1 minute. For staining purposes, it was then placed on a drop of uranyl acetate (2%) for 30 s. The solvent was evaporated before the stained grid was imaged. TEM images were elaborated using the software ImageJ (http:// rsb.info.nih.gov/ij/).

LSCM Analysis: Confocal images were taken using a laser scanning confocal microscope (BX51WI-FV300-Olympus) coupled to a frequency doubled Ti:Sapphire femtosecond laser at 400 nm, 76 MHz (VerdiV5Mira900-F Coherent). The laser beam was scanned on a 40x40 µm sample area with a 512x512 resolution, using a 60x water immersion objective (UPLSAPO60xW-Olympus).

1.2 Materials

All fine chemicals were sourced from commercial suppliers and were used directly without purification unless mentioned. The final solutions for analysis by UV-Vis and HPLC were prepared from stock solutions prepared in the respective solvent and diluted in MilliQ water.

ATP and adenosine were obtained from Sigma Aldrich. Solutions were prepared as an approximately 10 mM solution in MilliQ water by weight and the exact concentration was calculated by UV-Visspectroscopy using the molar extinction coefficients: ε_{259} (ATP, adenosine) = 15400 M^{-1} cm^{-1}.[49] Inorganic phosphate solution was prepared as a 20 mM stock solution by weight in MilliQ water.

The aldehydes *trans*-cinnamaldehydeand 2-pyridinecarboxylaldehydeand the hydrazide 3-hydroxy-2-napthoic hydrazide were purchased from Sigma Aldrich and used without further purification. Solutions were prepared by weight in acetonitrile at the required concentration, typically 20 mM, fresh before use. The concentrations wereconfirmed by UV-Vis spectroscopy using the molar extinction coefficients: ε (*trans*-cinnamaldehyde) = 25300 M^{-1} $cm^{-1(50)}$, ε (2-pyridinecarboxylaldehyde) = 5290 M^{-1} cm^{-1}.[51]

The concentration of the $Zn(NO_3)_2$-stock solution was quantified using EDTA following standard procedures.

The buffer 4-(2-hydroxyethyl)-1-piperazineethanesulfonic acid (HEPES) was procured from Sigma-Aldrich and used without further purification. The buffer were prepared as 100 mM solutions in MilliQ water and adjusted to a pH of 7.0.

The fluorophores DPH, 1,6-diphenyl-1,3,5-hexatriene and laurdan dye, 6-dodecanoyl-N,N-dimethyl-2-naphthylamine, were procured from Sigma-Aldrich andused without further purification.

The enzymealkaline phosphatase was obtained from Sigma Aldrich and used without further purification. The solution was diluted in 1 mL water to give a concentration of 1000 U/mL. The solution was further diluted to obtain a concentration of 100 U to be used for lower enzyme concentrations.

2. Synthesis and characterisation of the amphiphile C_{12}TACN

2.1 Synthesis and characterisation

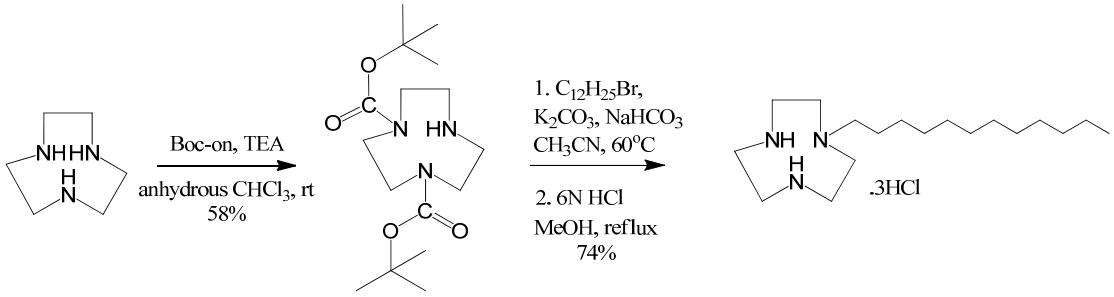

Scheme S1. Synthetic scheme for the synthesis of C_{12}TACN as the hydrochloride salt.

Di-tert-butyl 1,4,7-triazanonane-1,4-dicarboxylate (**b**) was synthesized from 1,4,7-triazanonane (**a**) according to a literature protocol (G. Pieters, A. Cazzolaro, R. Bonomi, L. J. Prins, Chem. Commun. 48, 1916 (2012)).

*1-Dodecyl-1,4,7-triazacyclononane (**C_{12}TACN.3HCl**)*: Compound **b** (0.20 g, 0.61 mmol) and dodecyl bromide (0.18 g, 0.71 mmol) were dissolved in 10 mL acetonitrile in a 50 mL round bottomed flask. $K_2CO_3.6H_2O$ (0.33 g, 2.0 mmol) and $NaHCO_3$ (0.22 g, 2.57 mmol) were added and the suspension was stirred at 60 °C for 9 hours. The mixture was subsequently filtered on gooch and the solvent evaporated under reduced pressure. The residual solid was then purified by silica flash chromatography using as eluent a solvent mixture of methanol and dichloromethane starting with 2% MeOH, which was gradually increased to 3% MeOH until the product was eluted and then increased to 10% MeOH to elute unreacted **b**. The protected C12 amphiphile was obtained as a pale, yellow oil (0.22 mg, 71%) and used directly in the next step. The obtained solid was dissolved in 7 mL MeOH in a 25 mL round-bottomed flask. A volume of 6 *N* HCl (6 mL) was added to the solution and the mixture was stirred for two hours at 60 °C. The solvent was evaporated under reduced pressure and the

solid was collected as a pinkish-white solid (120 mg, 74% yield). The solid was washed with cold chloroform to remove any organic residue.

^{1}H NMR (CD_3OD, 300 MHz, 300 K, ppm): δ 0.86 (m, 3H, CH_3), 1.20 (s, 18H, 9 × CH_2), 1.54 (s, 2H, CH_2), 2.75 (s, 2H, CH_2N), 2.99 (s, 4H,2 × CH_2N), 3.22 (s, 4H, 2 × CH_2N),3.45 (s, 4H, 2 × CH_2N).

^{13}C NMR (CD_3OD, 125 MHz, 300 K): δ 14.48, 23.78, 25.72, 28.46, 30.52, 30.65, 30.78, 33.12, 43.67, 44.83, 57.25

ESI-MS(ESI+, H_2O:CH_3CN = 1:1). *m/z* calculated for $C_{18}H_{39}N_3$: $[M+H]^+$ 298.3, found 298.3. N.B. The solid was preserved in the fridge. Prior to experiments, fresh solutions of amphiphile were prepared in small volumes as 10 mM solutions in milliQ water and preserved at room temperature to avoid aggregation and precipitation. The solutions were subsequently diluted to the required experimental concentration. The Zn^{2+} metal complex of C_{12}TACN was formed in situ by addingan equimolar quantity of $Zn(NO_3)_2$ to a buffered solution of the amphiphile.

2.2 Characterization data for C_{12}TACN

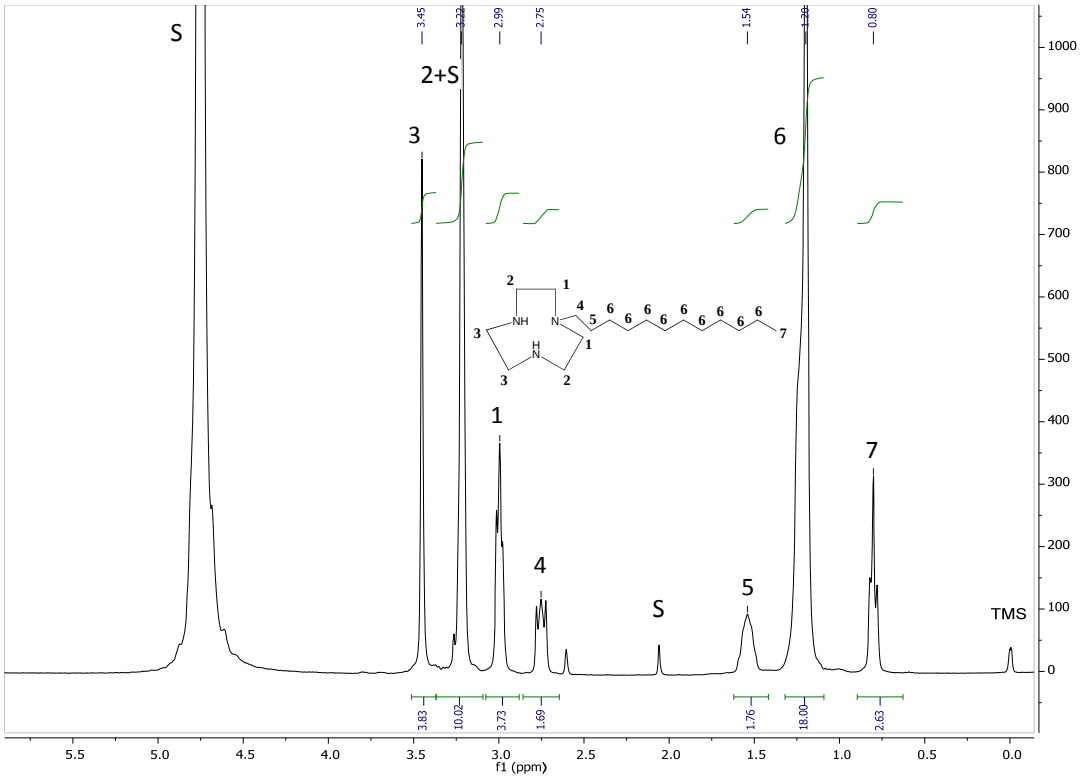

Figure S1. ^{1}H NMR spectrum of **C_{12}TACN** in MeOD (300 MHz, 300K). (S denotes solvent peaks.)

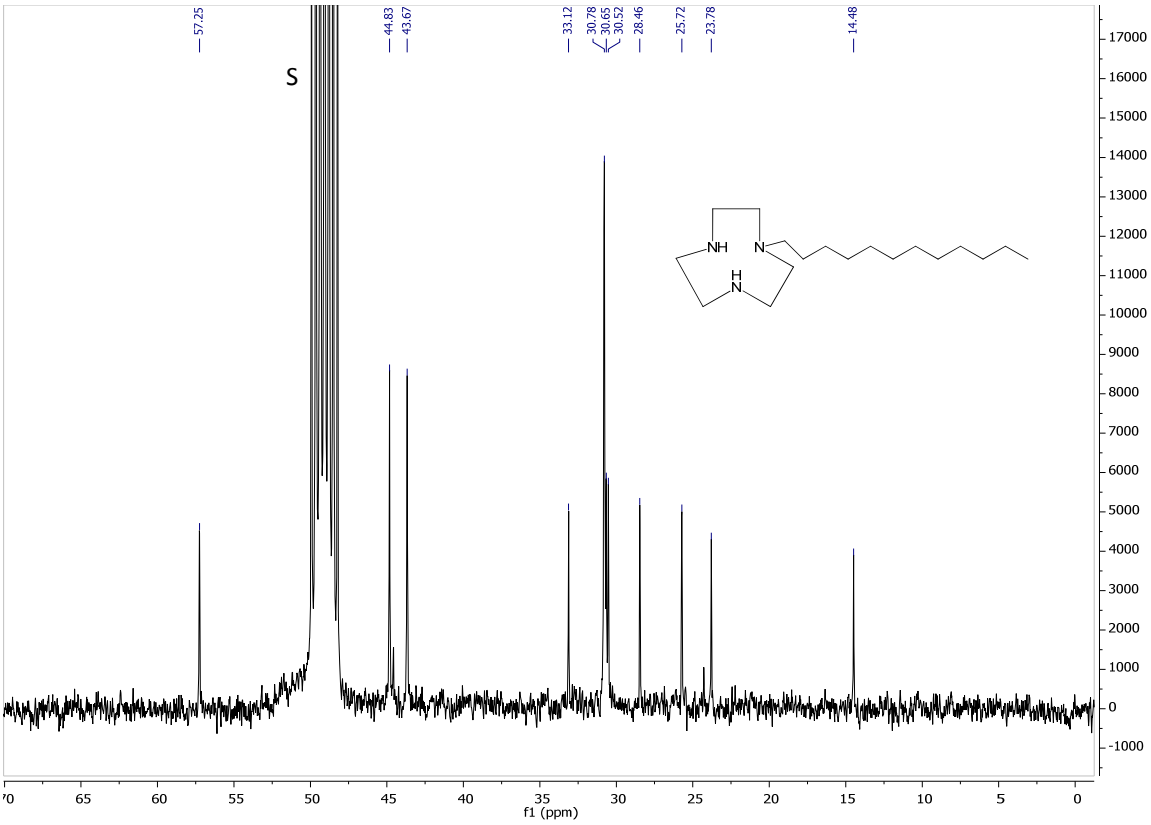

Figure S2. ^{13}C NMR spectrum of **C_{12}TACN** in MeOD (125 MHz, 300K).

3. ATP-templated self-assembly

3.1 ATP-assisted encapsulation of water-soluble dye Rhodamine 6G

Evidence for the presence of an aqueous interior phase in the assemblieswas obtained by encapsulation studies of the cationic water-soluble dye Rhodamine 6G (Rh6G). ATP (25 and 50μM) was added to a solution of C_{12}TACN·Zn^{2+} (100 μM) and Rhodamine 6G (1 μM). After an incubation period of 5 minutes, the samples were centrifuged for 45 minutes at 14000 rpm, resulting in the precipitation of the assemblies. The absorption spectrum of the supernatant was measured in order to quantify the amount of remaining dye in solution. In all cases, the remaining amount of Rh6G in the supernatant decreased. This indicated an uptake of the dye by the assemblies. The use of a cationic dye excluded that this was simply a result of electrostatic interactions with the (positively charged) amphiphile.

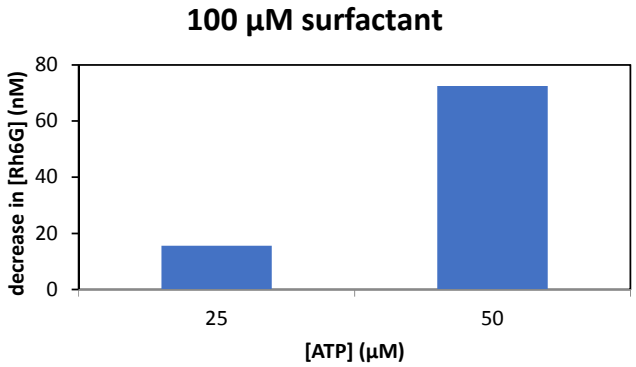

Figure S3. Decrease in Rh6G concentration in the supernatant as a function of ATP concentration for 100 µM C_{12}TACN•Zn^{2+}. [HEPES] = 5 mM, pH 7.0, [Rh6G] = 1 µM, centrifugation speed = 14000 rpm, centrifugation time = 45 minutes.

4. Chemical reactivity in self-assembled assemblies

4.1 Synthesis and characterisation of hydrazones

Hydrazones were synthesized using general published procedures.[3] Generally, the solid hydrazide was dissolved in a minimal amount of ethanol in a round-bottomed flask and the solution was stirred with a magnetic stirrer. An equimolar quantity of the respective aldehyde was added dropwise to the solution whilst stirring the solution. A few drops of TFA were sometimes added as a catalyst. The hydrazones precipitated out of solution as white or yellow solids, which were filtered and if necessary, recrystallised from methanol.

The identity and purity of all hydrazones were confirmed by ^{1}H and ^{13}C NMR spectroscopy and ESI-MS. When obtained in DMSO-d_6, the NMR spectra of the hydrazones generally showed the presence of two isomers.[3] On the other hand, only one isomer was observed when the ^{1}H NMR spectrum of the product was obtained in CD_3OD.

Hydrazone 1A: Hydrazone **1A**was synthesized from 383 mg (1.89 mmol) 3-hydroxy-2-napthoic hydrazide and 294 mg (2.22 mmol) *trans*-cinnamaldehydein 50 ml absolute ethanol. The solid crystallised out upon concentration of solution and recrystallised from ethanol to give 314 mgof **1A** (52.5% yield).

R_f = 0.5 (hexane:ethyl acetate 80:20)

UV-Vis: λ_{max} = 331 nm (methanol)

^{1}H NMR (only major isomer: 88%) (DMSO-*d6*, 300 MHz, 300 K, ppm): δ 7.08 (d, *J* = 4.3 Hz, 2H), 7.25 – 7.41 (m, 6H), 7.48-7.50 (m, 1H), 7.62 (d, *J* = 7.4 Hz, 2H), 7.73 (d, *J* = 8.3 Hz, 1H), 7.87 (d, J = 8.3 Hz, 1H), 8.21-8.23 (m, 1H), 8.41 (s, 1H), 11.28 (s, 1H), 11.85 (s, 1H)

^{1}H NMR (MeOD-*d*$_4$, 300 MHz, 300 K, ppm): δ 7.10 (d, *J* = 4.3 Hz, 2H), 7.29 – 7.40, (m, 6 H), 7.45-7.55 (m, 1H), 7.55-7.64 (m, 2H), 7.70 (d, *J*= 8.3 Hz, 1H), 7.88 (d, *J* = 8.3 Hz, 1H), 8.18 – 8.20 (m, 1H), 8.52 (s, 1H)

^{13}C NMR (DMSO-*d6*, 126 MHz, 300 K, ppm): δ 111.02, 120.77, 124.27, 125.97, 126.32, 127.25, 127.67, 128.70, 129.14, 129.35, 129.46, 130.71, 136.31, 140.13, 150.97, 154.57, 164.17

MS (ESI,+, MeOH:H_2O 1:1): m/z calculated for $C_{20}H_{16}N_2O_2$: $[M+H]^+$: 317.3, found 317.2.

HPLC-MS (λ = 331 nm): R_t = 4.3 minutes

Hydrazone 2A: Hydrazone **2A**was synthesized from 254 mg (1.25 mmol) 3-hydroxy-2-napthoic hydrazide and 135 mg (1.25 mmol) pyridine carboxylaldehyde in 150 mL absolute ethanol. The orange-yellow solid precipitated out of solution upon evaporation of some of the solution, was filtered, dried and recrystallised from methanol to afford 128 mg of **2A**(35% yield).

UV-Vis: λ_{max} = 329 nm

^{1}H NMR (only major isomer: 86%) (DMSO-*d6*, 300 MHz, 300 K, ppm): δ 7.21 – 7.55 (m, 4H), 7.74 (d, *J* = 8.1 Hz, 1H), 7.89 (d, *J* = 7.2 Hz, 2H), 8.00 (d, *J* = 8.1 Hz, 1H), 8.40 - 8.44 (m, 2H), 8.62 (s, 1H), 11.10 (s, 1H), 12.11 (s, 1H).

^{13}C NMR (DMSO-*d6*, 126 MHz, 300 K, ppm): δ 110.97, 120.57, 121.34, 124.29, 125.04, 126.34, 127.26, 127.37, 128.71, 129.12, 130.77, 136.31, 137.43, 148.96, 150.07, 153.61, 154.33, 164.49

MS (ESI,+, MeOH:H_2O 1:1): m/z calculated for $C_{17}H_{13}N_3O_2Na$: $[M+Na]^+$ 314.2, found 314.1.

HPLC-MS (λ = 331 nm): R_t = 3.4 minutes

4.2 ^{1}H NMR and^{13}C NMR spectra

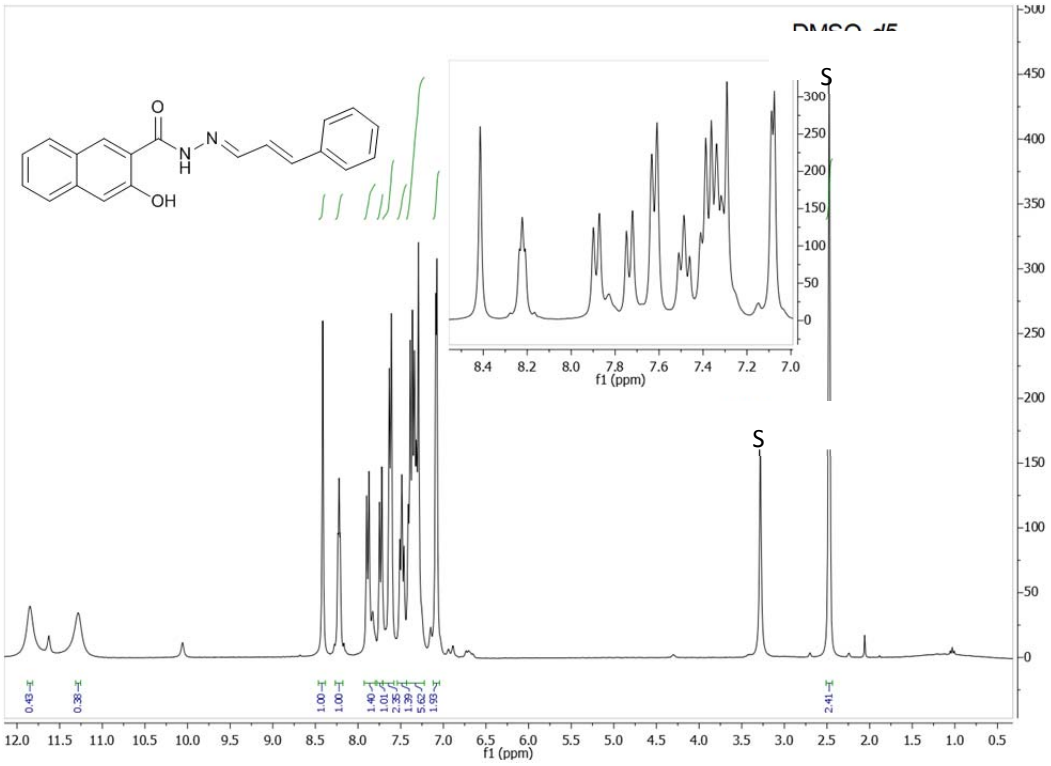

Figure S4.^{1}H NMR spectrum of **1A**in DMSO-*d6* (300 MHz, 300K).

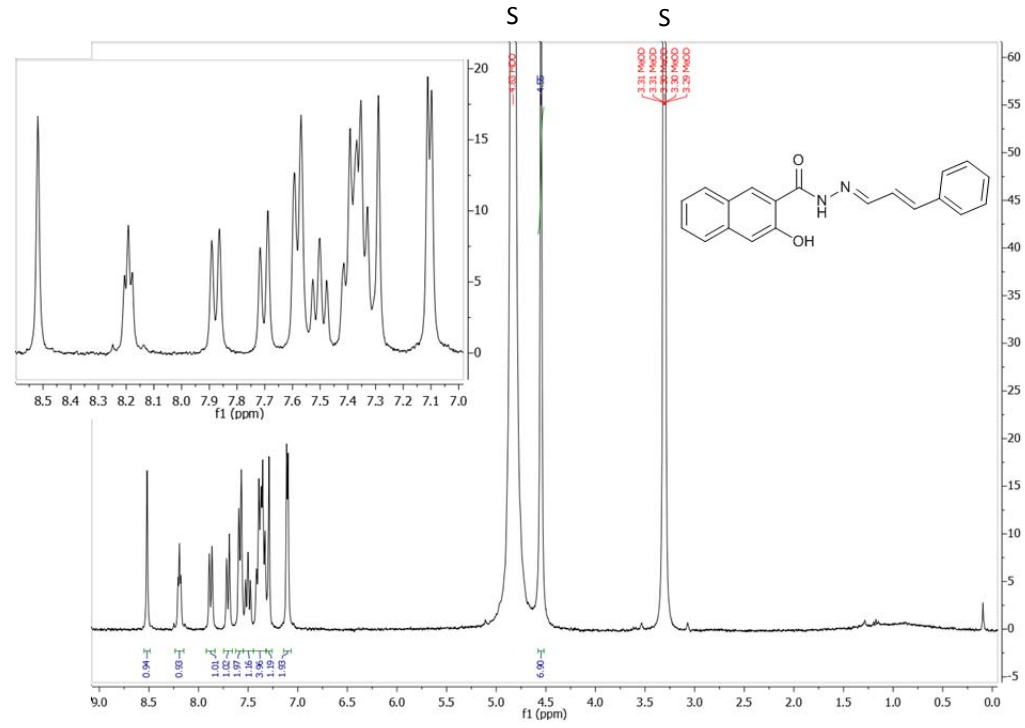

Figure S5.^{1}H NMR spectrum of**1A** in MeOD (300 MHz, 300K).

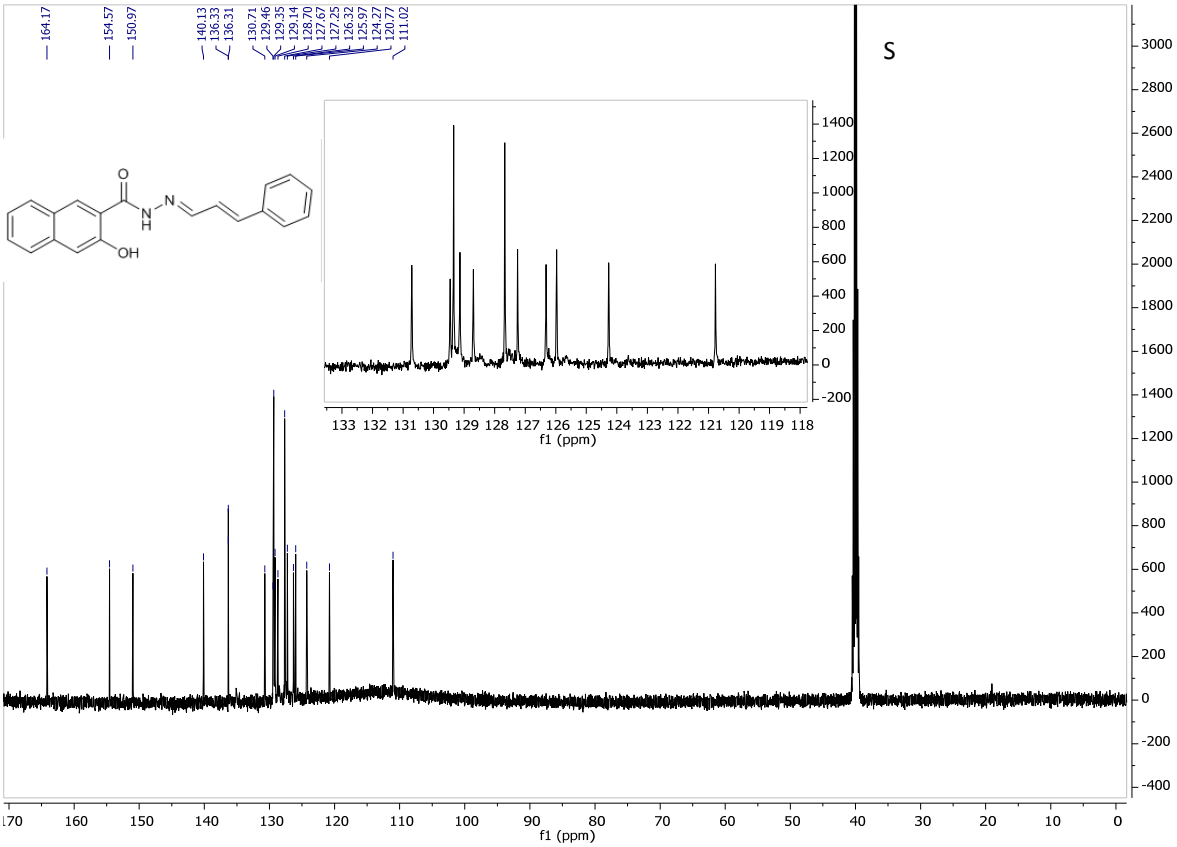

Figure S6. ^{13}C NMR spectrum of **1A** in DMSO-*d6* (126 MHz, 300K).

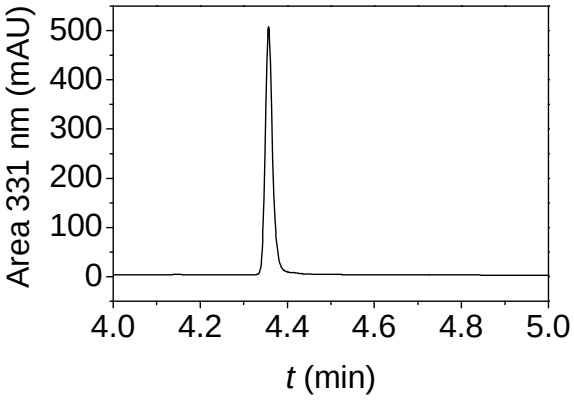

Figure S7. HPLC chromatogram of **1A**(20 μM) monitored at 331 nm. Retention time: 4.3 min. A volume of 2 μL of the stock solution of the compound (in DMSO-*d6*, 10 mM) was added to an aqueous buffered solution (HEPES, 5 mM, pH 7) of 1 mL.Conditions: Flow rate: 0.6 ml/min, Gradient: 5-95 %B to 95-5%B (A: H_2O+0.1%HCOOH, B: ACN+0.1% HCOOH) in 0.00 to 5.00 min; 95-100 % B in 5 to 5.10 min; 100 % B from 5.10 to 8.10 min; 100-5 % B in 8.10 to 9.10 min; and finally 5% B from 9.10 to 10.00 min. Column: Agilent Zorbax SB-C3 Rapid Resolution HT 3.0 × 100 mm 1.8 micron. Injection volume: 20 μL Column temperature: 40 ^{o}C.

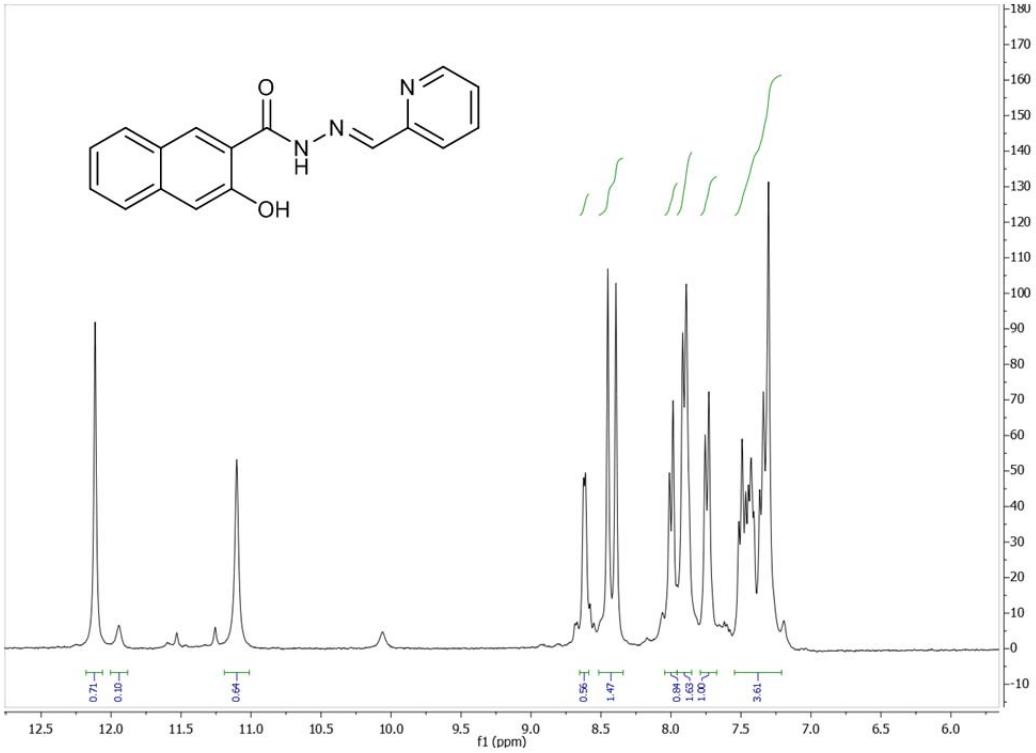

Figure S8.[1]H NMR spectrum of **2A** in DMSO-*d6* (300 MHz, 300K).

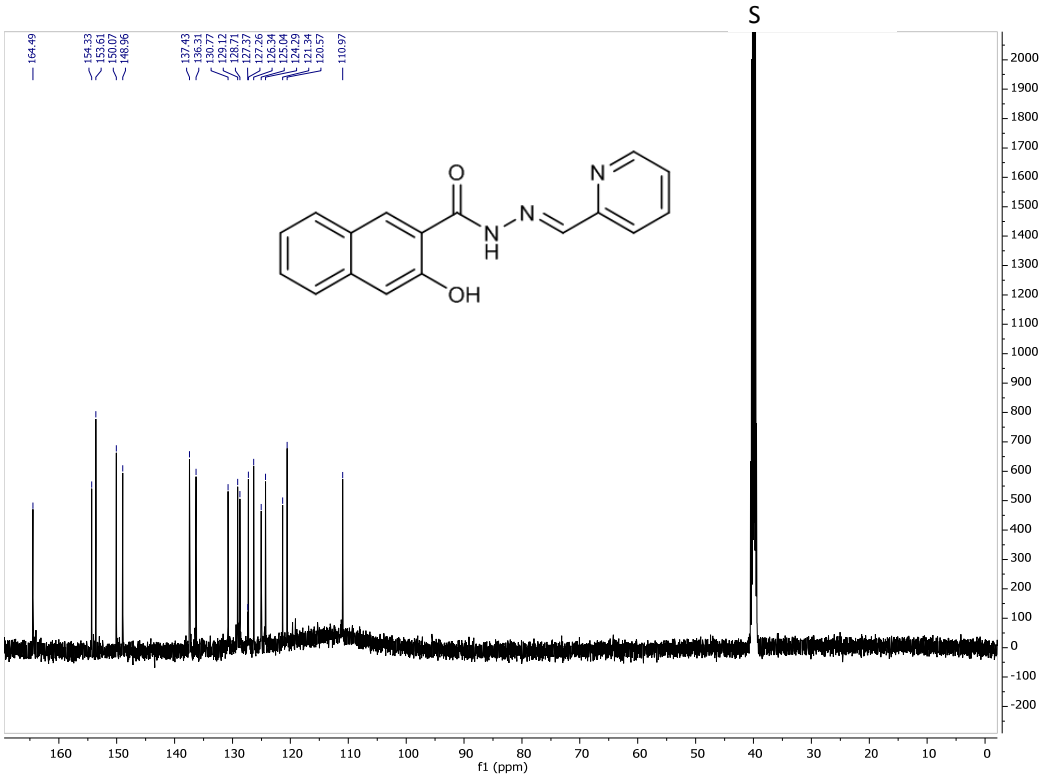

Figure S9.[13]C NMR spectrum of**2A** in DMSO-*d6* (126 MHz, 300K).

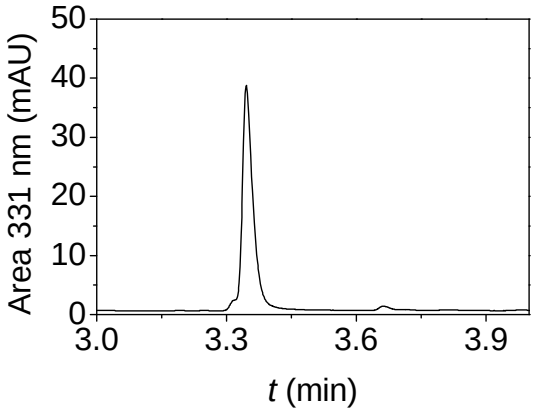

Figure S10. HPLC chromatogram of **2A**(20 μM) monitored at 331 nm nm. Retention time: 3.4 min. 2 μL of the stock solution of the compound (in DMSO-*d6*, 10 mM) was added to an aqueous buffered solution (HEPES, 5 mM, pH 7) of 1 mL.Conditions: Flow rate: 0.6 ml/min, Gradient: 5-95 %B to 95-5%B (A: H_2O+0.1%HCOOH, B: ACN+0.1% HCOOH) in 0.00 to 5.00 min; 95-100 % B in 5 to 5.10 min; 100 % B from 5.10 to 8.10 min; 100-5 % B in 8.10 to 9.10 min; and finally 5% B from 9.10 to 10.00 min. Column: Agilent Zorbax SB-C3 Rapid Resolution HT 3.0 × 100 mm 1.8 micron. Injection volume: 20 μL Column temperature: 40 ^{o}C.

4.3 Quantification of the concentrations (UV-Vis and HPLC)

The stock solutions of reactants were prepared in acetonitrile to ensure adequate solubility. Mixing the reactants in buffer, amphiphile and vesicles resulted in the formation of a tiny fraction of product at the starting time-point. This effect was probably due to the small percentage of organic solvent in the solution. In cases where reactions needed to be compared, the values were normalised for the initial quantity of product formed upon mixing. The exact concentration of the aldehydes was determined by UV-Vis spectroscopy. The reagent solutions were prepared fresh prior to each experiment.

The corrected absorbance obtained by UV-Vis spectroscopy and the integrated area obtained by HPLC at the appropriate wavelength were converted to concentration using the appropriate calibration curves in the appropriate solvent. Solutions were prepared with the reagents at different concentration and the absorbance at the λ of analysis or the area under the peaks at the appropriate wavelength was plotted against the concentration. The slope of the linear curve thus obtained was used to determine the ε in the case of UV-Vis measurements and the conversion factor in the case of the HPLC measurements.

4.3.1 Calibration curves for hydrazone 1A by UV-Vis Spectroscopy

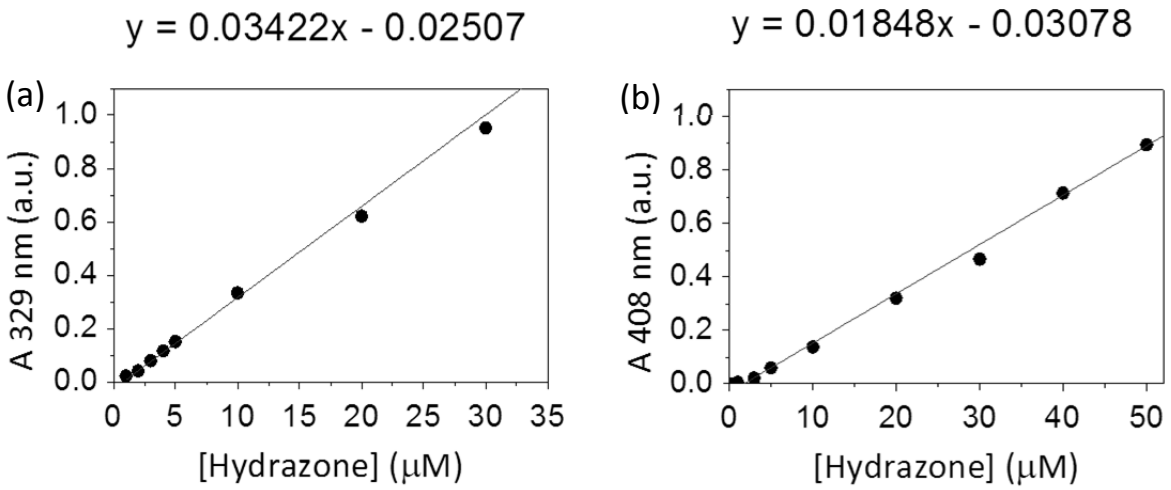

Figure S11. Calibration curve for hydrazone **1A** in (a) HEPES buffer pH 7.0 monitoring the λ_{max} peak at 329 nm and (b)200 μM $C_{12}TACN{\cdot}Zn^{2+}$ monitoring the λ_{max} peak at 408 nm. [HEPES] = 5 mM, pH 7.0.

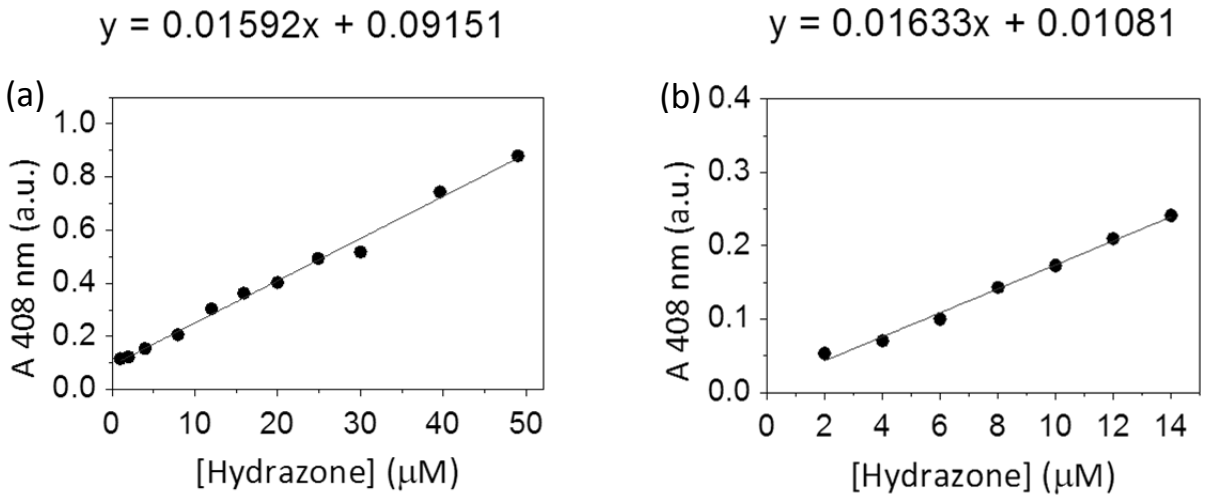

Figure S12. Calibration curve for hydrazone **1A** in 200 μM amphiphile**10**, 200 μM ATP at pH 7.0 monitoring the λ_{max} peak at 408 nm.The two graphs show two different concentration ranges. [HEPES] = 5 mM, pH 7.0.

4.3.2 Calibration curves for hydrazone 1A by HPLC

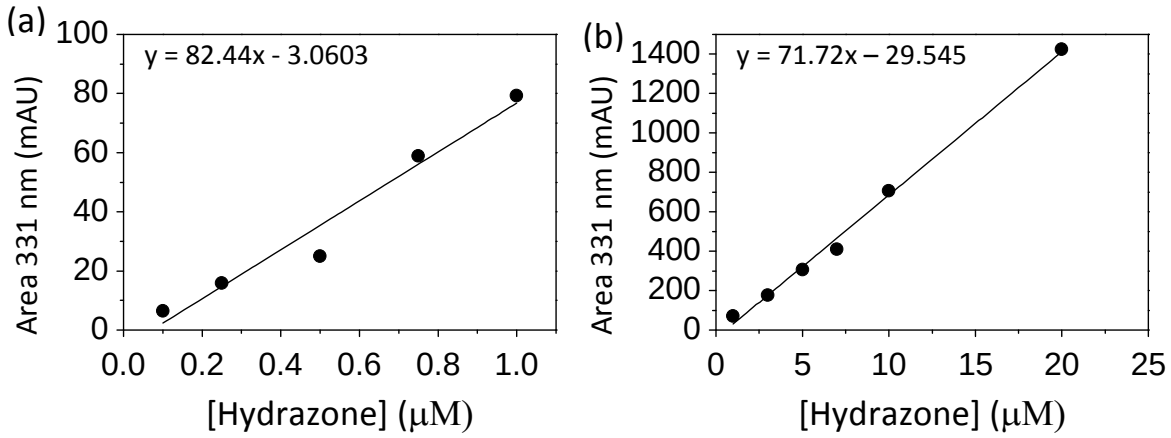

Figure S13. Calibration curve for hydrazone**1A**in HEPES buffer pH 7.0 (a) between 0-1 μM and (b) between 0-25μM**.** [HEPES] = 5 mM, pH 7.0.

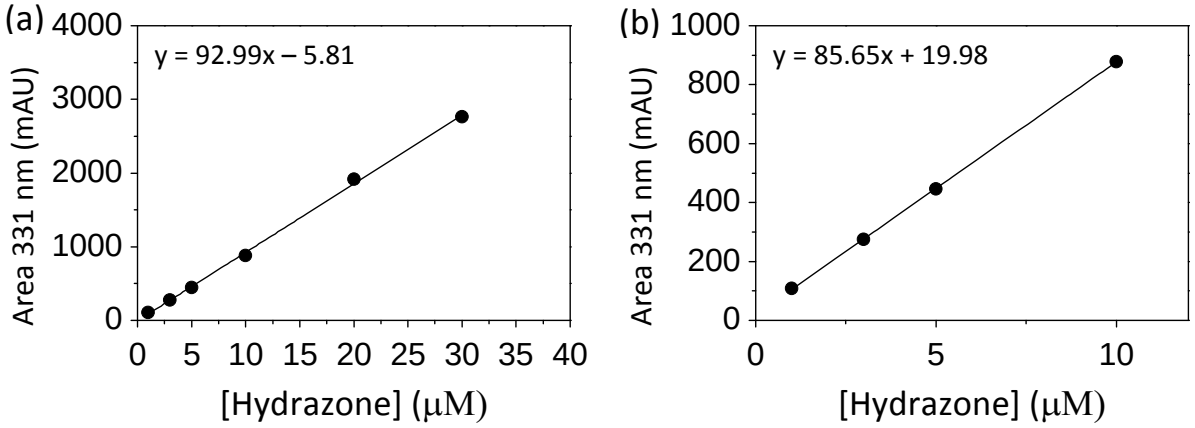

Figure S14. Calibration curves for hydrazone **1A** in acetonitrile, monitoring the area of the hydrazone peak at 331 nm.[HEPES] = 5 mM, pH 7.0.

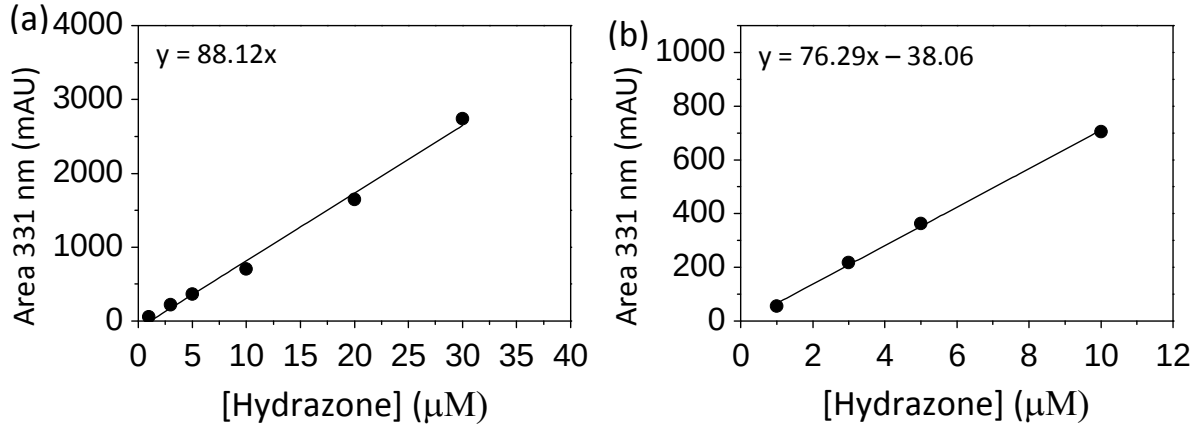

Figure S15. Calibration curves for hydrazone **1A** in 100 μM $C_{12}TACN{\cdot}Zn^{2+}$, monitoring the area of the hydrazone peak at 331 nm. [HEPES] = 5 mM, pH 7.0.

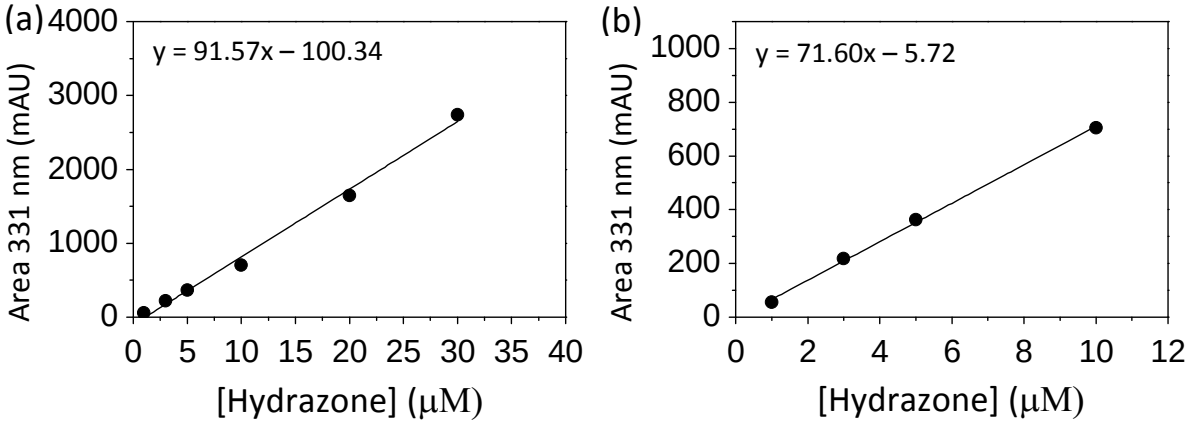

Figure S16. Calibration curves for hydrazone 1A in 100 μM $C_{12}TACN{\cdot}Zn^{2+}$, 200 μM ATP (assemblies), monitoring the area of the hydrazone peak at 331 nm. [HEPES] = 5 mM, pH 7.0.

4.3.3 Calibration curves for hydrazone 2A by HPLC

Calibration curves were prepared separately for the hydrazone **2A** in buffer, in 100 μM $C_{12}TACN{\cdot}Zn^{2+}$ and for assemblies obtained from mixing 200 μM ATP with 100 μM $C_{12}TACN{\cdot}Zn^{2+}$ at five different concentrations. They were injected in the HPLC and the area of **2A**was plotted against the concentration. Linear regression of the plots gave an equation which was used to change the area into concentration.

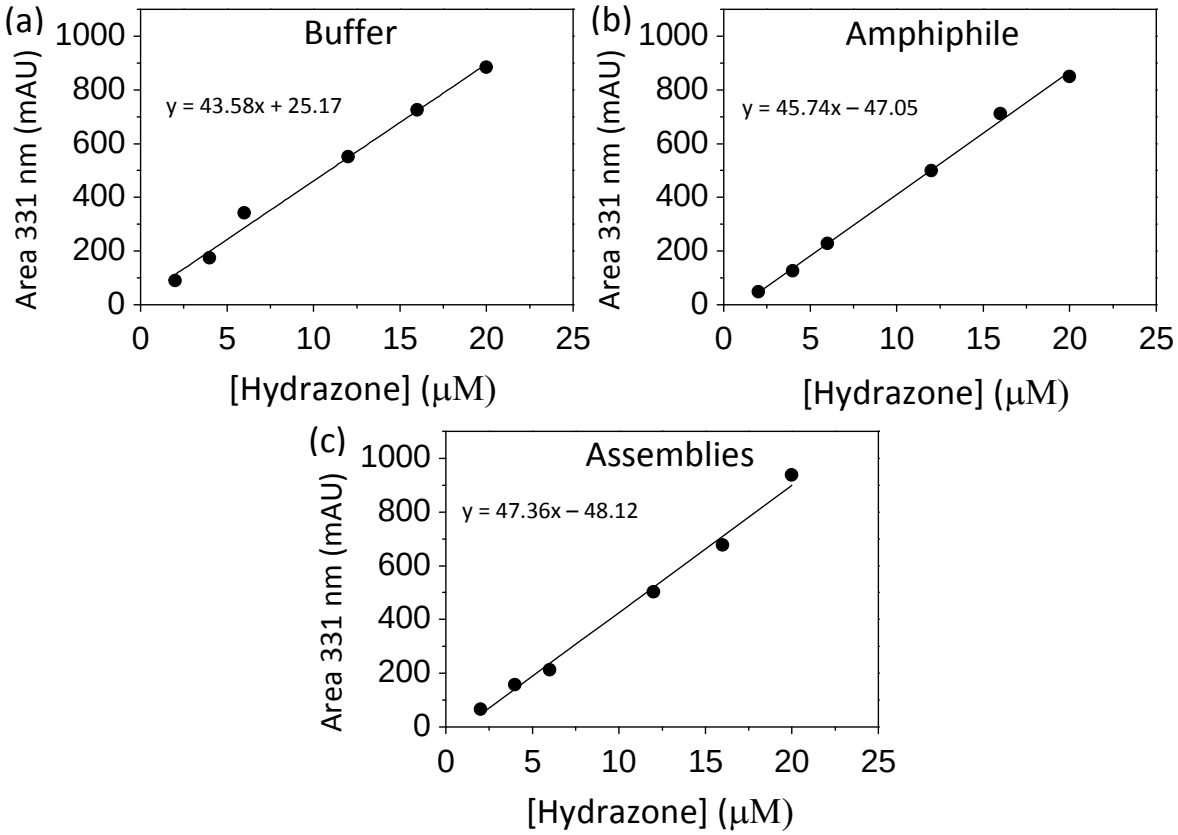

Figure S17. Calibration curves showing plots of the intergrated area against the concentration of **2A** for standard solutions in (a) aqueous buffer, (b) 100 μM $C_{12}TACN{\cdot}Zn^{2+}$ and (c) 100 μM $C_{12}TACN{\cdot}Zn^{2+}$, 200 μM ATP. [HEPES] = 5 mM, pH 7.0.

4.4 UV-Vis spectra of 1 and 1A

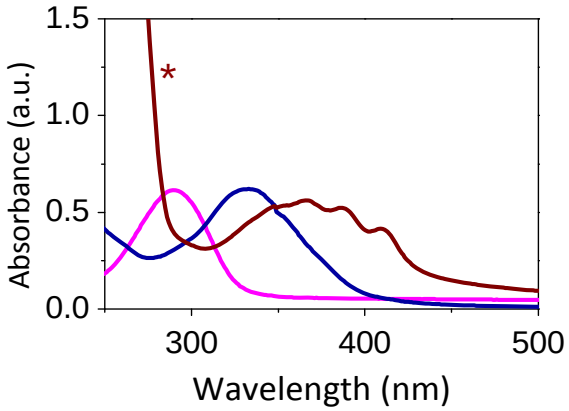

Figure S18.UV-Vis spectra of **1** (20 μM, pink) and **1A** (20 μM) in aqueous buffer at pH 7.0 (blue) or in the presence of C_{12}TACN·Zn^{2+} (100 μM) and ATP (200 μM) (red - * denotes the absorption band from ATP).

4.5 TEM and DLS in the presence of reagents

The figure below shows the TEM of the aggregates formed from the surfactant and ATP in the presence of **1** (a) and **1** and **A** after 8 hours (i.e. in the presence of product). The figure shows that the structure is preserved in all three cases.

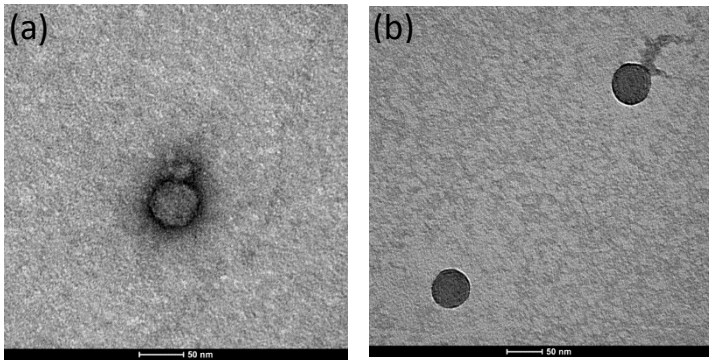

Figure S19. (a) TEM image of aggregates with [C_{12}TACN•Zn^{2+}] = 100 μM, [ATP] = 200 μM and [**1**] = 20 μM. (b) TEM image of aggregates with [C_{12}TACN•Zn^{2+}] = 100 μM, [ATP] = 200 μM and [**1**] = [**A**] = 20 μM after 8 hours (i.e. containing **1A**). The scale bar corresponds to 50 nm.

4.6 Kinetics of formation of 1A by UV-Vis and HPLC

Figure S20a shows the kinetics of formation of **1A** as determined by HPLC when 20 μM **1** and **A** were reacted in the presence of 100 μM C_{12}TACN•Zn^{2+} and increasing concentrations of ATP. The linear part of the curve (typically the first three points) was used to calculate the initial rate of reaction at each ATP concentration. The values obtained were plotted against ATP concentration as shown in Figure S20b. Plotting ln v_o against ln [ATP] (Figure S21) gave an order of reaction of 0.9.

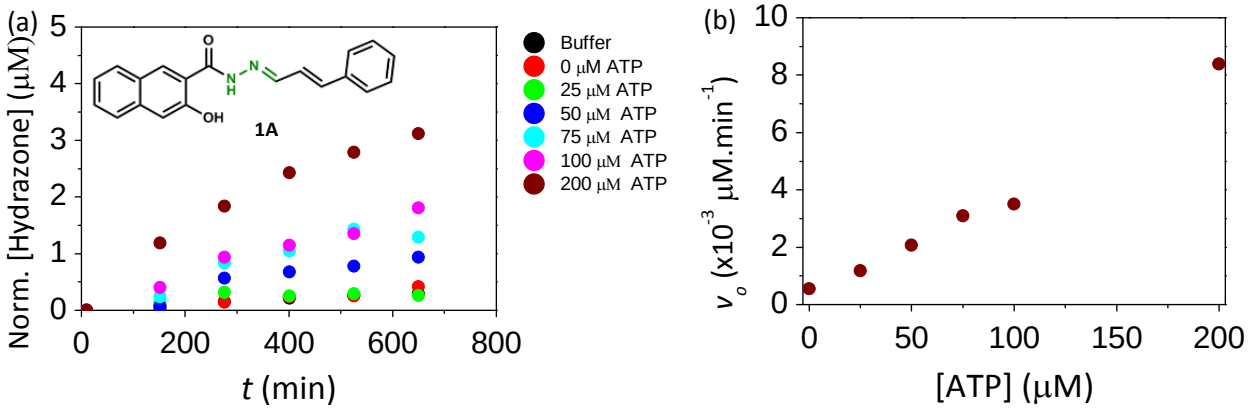

Figure S20.(a) Graph showing the increase in the concentration of **1A**when carrying out the reaction between **1** and**A** in the presence of 100 μM C_{12}TACN•$Zn^{2+}$and increasing concentrations of ATP. Graphs are plotted from the same experiment. (b) Initial rate of formation of **1A** as a function of concentration of ATP determined from graph (a).[HEPES] = 5 mM, pH 7.0, [C_{12}TACN•Zn^{2+}] = 100 μM, [**1**] = [**A**] = 20 μM.

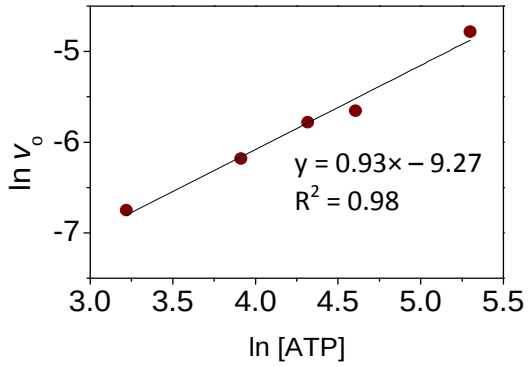

Figure S21. A plot of ln initial rate against ln [ATP]. The gradient of the straight line graph gave the order of reaction (0.9).

Figure S22 compares the kinetics of formation of **1A** in HEPES buffer pH 7.0, 100 µM C_{12}TACN·Zn^{2+} and in assemblies formed from 100 µM C_{12}TACN·Zn^{2+}, 200 µM ATP. The top graph shows the kinetic traces while the graphs below shows the UV-Vis spectra over time under the different conditions. Figure S23 shows the same experiment followed withHPLC-MS. Figure S24 shows the MS of the product peak with a retention time of 3.9 minutes, with an m/z value of 317 g/mol [M+H].

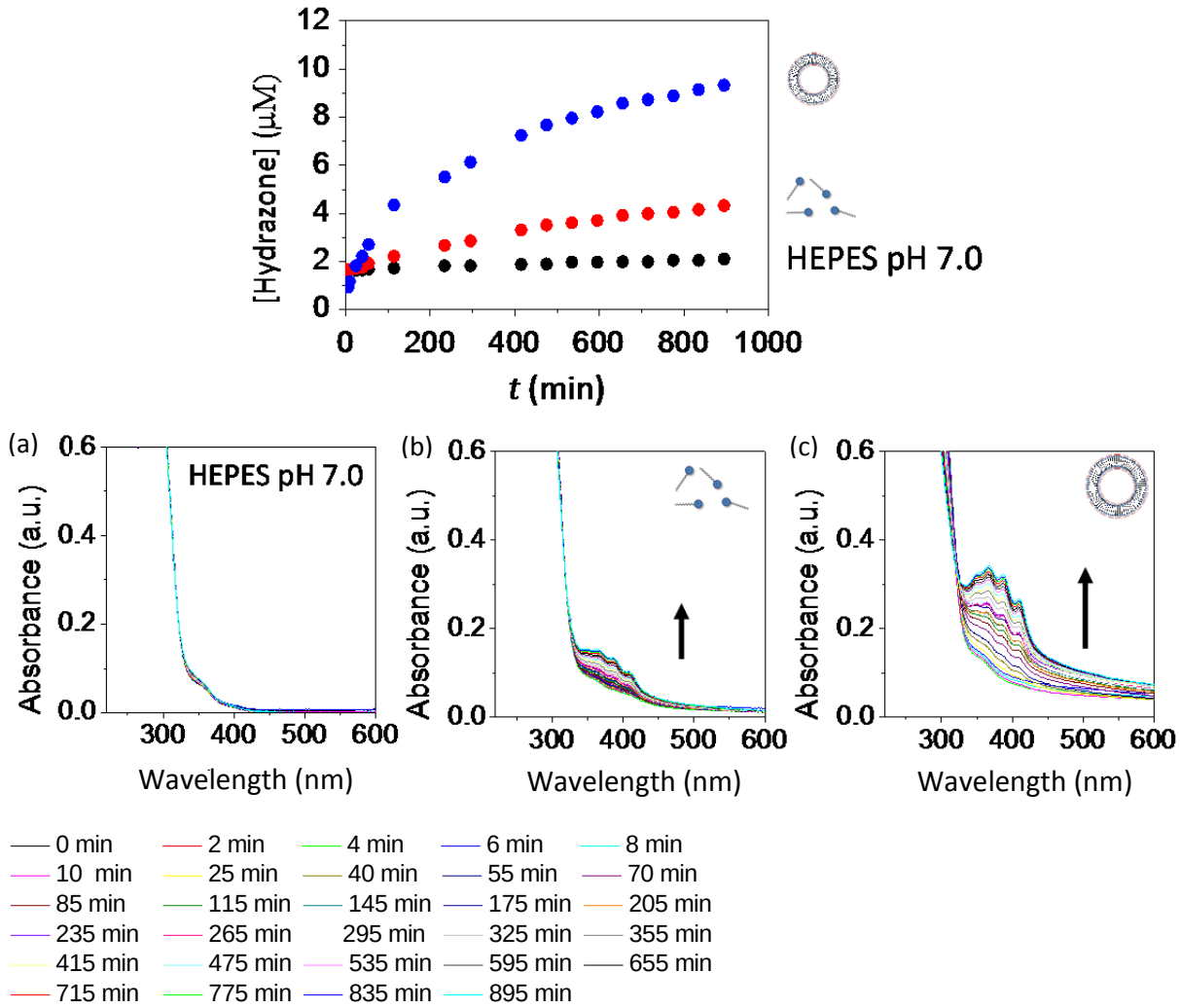

Figure S22. Concentration of hydrazone **1A** as a function of time (top) and UV-Vis spectra at regular intervals (bottom) of the reaction of 20 µM reagents in (a) aqueous buffer (b) C_{12}TACN·$Zn^{2+}$and (c) assemblies.[HEPES] = 5 mM, pH 7.0, [C_{12}TACN·Zn^{2+}] = 100 µM, [ATP] = 200 µM, [**1**] = [**A**] = 20 µM.

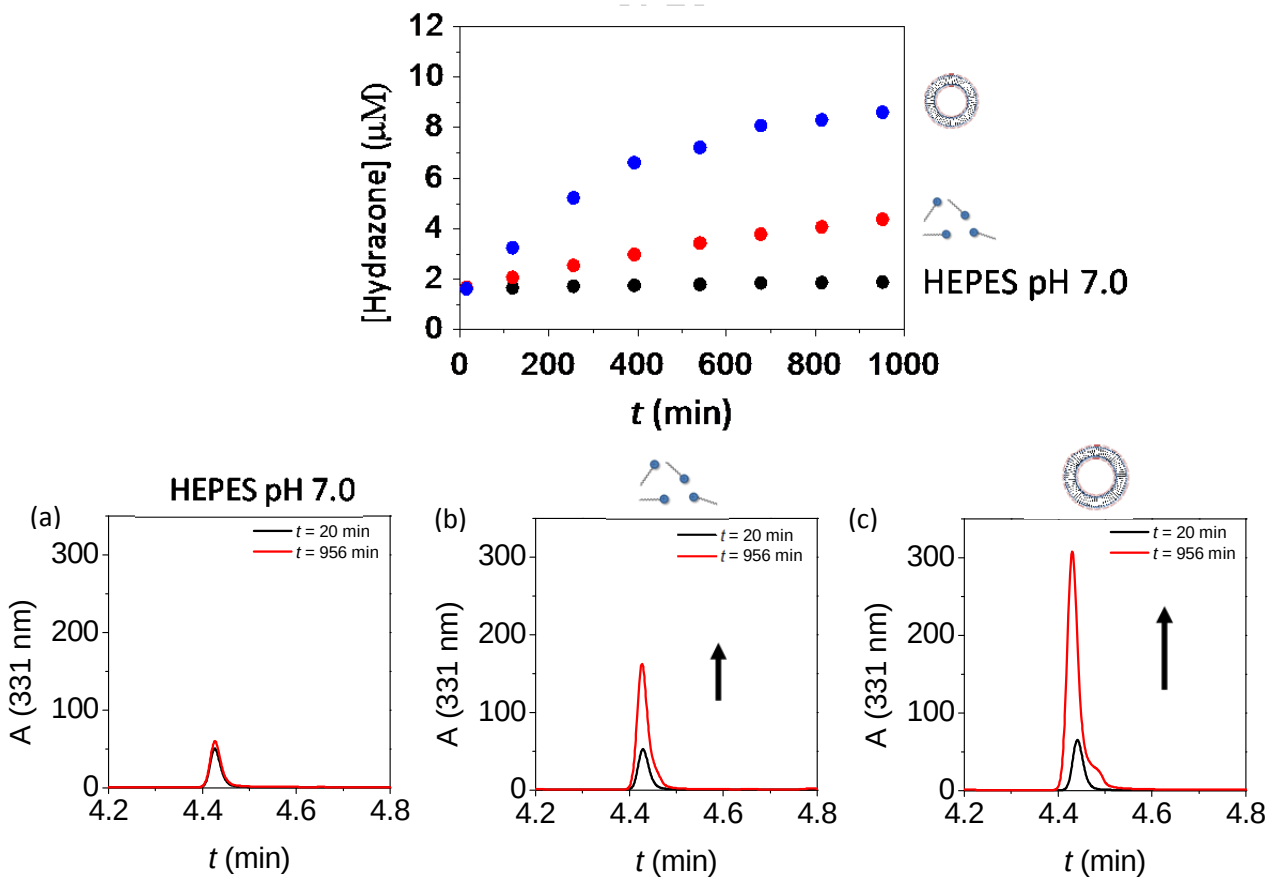

Figure S23. Concentration of hydrazone **1A** as a function of time (top) and HPLC chromatograms (initial and final) (bottom) of the reaction of 20 μM reagents in (a) aqueous buffer (b) C_{12}TACN·$Zn^{2+}$and (c) assemblies. [HEPES] = 5 mM, pH 7.0, [C_{12}TACN·Zn^{2+}] = 100 μM, [ATP] = 200 μM, [**1**] = [**A**] = 20 μM.

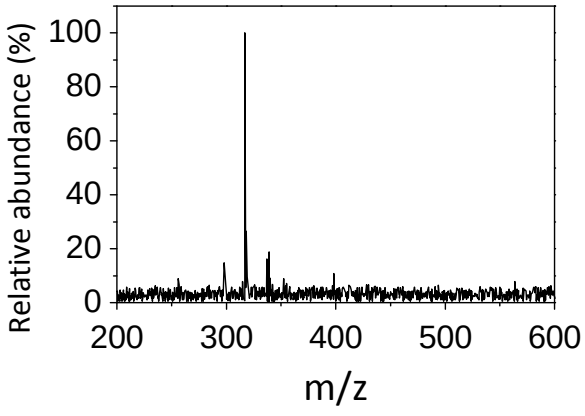

Figure S24. MS-spectrum of the product peak formed when **1** and **A** were reacted in assemblies [HEPES] = 5 mM, pH 7.0, [C_{12}TACN·Zn^{2+}] = 200 μM, [**1**] = 5 μM, [**A**] = 25 μM.
MS (ESI,+, MeOH:H_2O 1:1): m/z calculated for $C_{20}H_{16}N_2O_2$ [M+H]+ 317.3; found 317.2.

Figure S25 shows the control experiment in which ATP was added to the buffer in the presence of $C_{12}TACN{\cdot}Zn^{2+}$ by UV-Vis. There was no evidence of product formation over time.

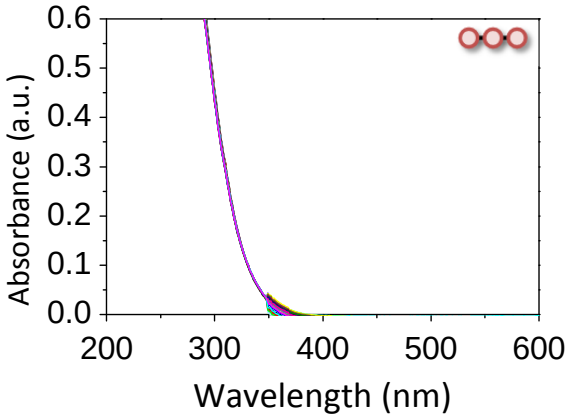

Figure S25.(a) UV-Vis spectra at regular intervals of the reaction of 20 μM reagents in 200 μM ATP. [HEPES] = 5 mM, pH 7.0 [**1**] = [**A**] = 20 μM.

4.7 Reactivity of 1A and 2A in the presence of the enzyme alkaline phosphatase

Figure S26 shows the kinetic traces obtained when hydrazones **1A** and **2A** were formed from solutions of their respective reactants (20 μM) in the presence of $C_{12}TACN{\cdot}Zn^{2+}$ (100 μM) and the enzyme alkaline phosphatase (0.5 U) upon repeated addition of 50 μM aliquots of ATP. The formation reactions were carried out in separate vials for the two reactants. A separate experiment was carried out in the absence of reactants but in the presence of laurdan dye (2 μM) in order to monitor the formation and degradation of the assemblies by fluorescence spectroscopy.

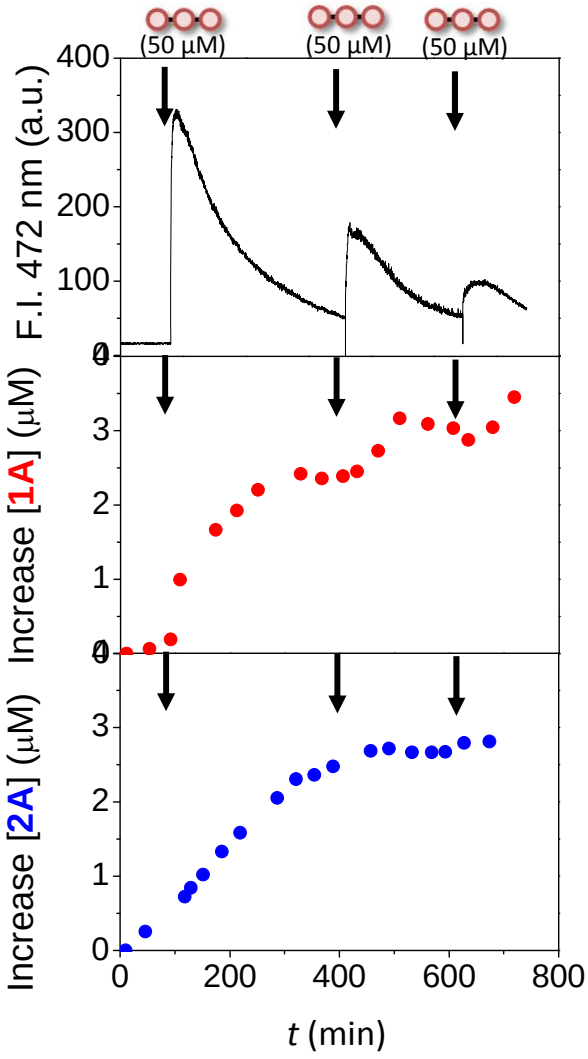

Figure S26.(a) Figure showing the F.I. of laurdan dye in 100 µM surfactant and 0.5 U alkaline phosphase and upon repetitive addition of 50 µM ATP. (b) Figure showing the concentration of **1A** in 100 µM surfactant and 0.5 U alkaline phosphase and upon repetitive addition of 50 µM ATP. (c) Figure showing the concentration of hydrazone **2A** in 100 µM surfactant and 0.5 U alkaline phosphatase and upon repetitive addition of 50 µM ATP. λ_{ex} = 370 nm, Slits = 5/10 nm (ex/em), 25 ^{o}C, [HEPES] = 5 mM, pH 7.0, [Laurdan] = 2 µM, [Surfactant] = 100 µM, [ATP] = 50 µM, [alkaline phosphatase] = 2 U, [1] = [2] = 20 µM, [A] = 40 µM.

4.8 Control of reactivity of hydrazones 1A and 2A by controlling the self-assembly

The different response of the two reactions to the absence or presence of templated assemblies were also assessed by first carrying out the reactions in HEPES buffer pH 7.0 and ATP. ATP on its own did not effect product formation and under these conditions, the formation of **2A** was much more favoured than that of **1A**. Addition of $C_{12}TACN{\cdot}Zn^{2+}$ (100

μM) at around 450 minutes, however, led to a strong enhancement in the rate of formation of **1A** but did not significantly affect the formation of **2A**. Consequently the formation of **1A** became the preferred reaction after some time (Figure S27).

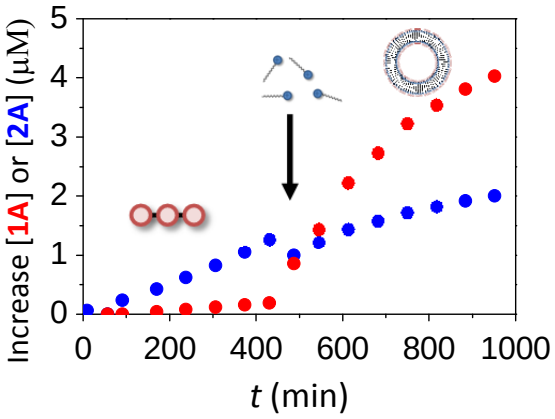

Figure S27. Graph showing the increase in **1A** and **2A** in aqueous buffer and ATP and upon addition of $C_{12}TACN{\cdot}Zn^{2+}$ to form assemblies. [$C_{12}TACN{\cdot}Zn^{2+}$] = 100 μM, [ATP] = 200 μM, [**1**] = [**2**] = [**A**] = 20 μM.

The following is a duplicate experiment for the final experiment in which ATP is added to a solution containing reagents **1**, **2** and **A**, $C_{12}TACN{\cdot}Zn^{2+}$ and the enzyme alkaline phosphatase (AP) under optimized conditions in terms of concentration.

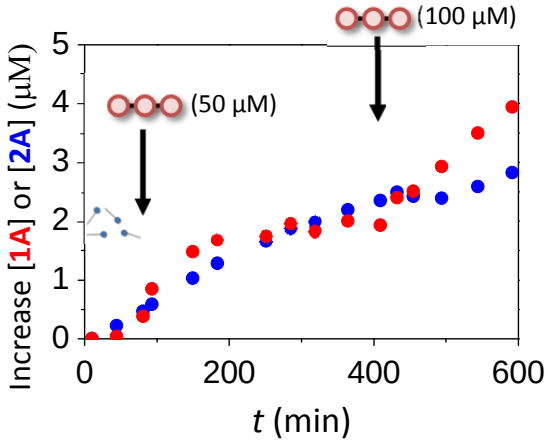

Figure S28. Duplicate experiment showing the increase in concentration of **1A** and **2A** over time when a mixture of **1** (20 μM), **2** (20 μM) and **A** (40 μM) were added to a solution of $C_{12}TACN{\cdot}Zn^{2+}$ (100 μM) and alkaline phosphatase (0.5 U) and to which ATP (50 μM) was added at different times. [HEPES] = 5 mM, pH 7.0, [$C_{12}TACN{\cdot}Zn^{2+}$] = 100 μM, [ATP] = 50 μM, 100 μM, [alkaline phosphatase] = 0.5 U, [**1**] = [**2**] = 20 μM, [**A**] = 40 μM.

5. Kinetic model

A kinetic model was developed to simulate ATP-regulated product formation. The ATP-induced transition from an unassembled to an assembled state is treated as 1:1 complex formation between surfactant and ATP under saturation conditions. This implies that the addition of ATP quantitatively converts surfactant in vesicles. Evidently, this does not correspond to reality, but from a modelling point of view it is the most effective way to describe a transition between two states.

The rate of hydrazone bond formation depends on the assembly state of the surfactant. For each hydrazone **1A** and **1B** these rates were determined both in the assembled and unassembled state by fitting the data reported in Figure 3b+d of the manuscript. The obtained rates were overall rates including the – possible – background reaction. To permit a smooth transition of the rate from the assembled to the non-assembled state (and back) under dissipative conditions, the surfactant (or vesicle) concentration were always included in the rate equation. ATP hydrolysis was described using first order decay kinetics.

The addition of ATP after a certain time interval was simulated by taking the calculated concentrations of the system prior to ATP-addition as input values for a new simulation in the presence of ATP.

The model was implemented in MicroMath Scientist for Windows (version 2.01).

```
// MicroMath Scientist Model File
IndVars: T
DepVars: H1A, H2A, V, S, ATP, H1, H2, A, H1TOT, H2TOT, ATOT
Params: ka, kd, kcat, k1s, k1v, k2s, k2v, V0, S0, ATP0, H1A0, H2A0, H10,
H20, A0
V'=ka*S*ATP-kd*V
S'=-ka*S*ATP+kd*V
ATP'=-ka*S*ATP+kd*V-kcat*ATP
H1A'=k1s*S*H1*A+k1v*V*H1*A
H1'=-k1s*S*H1*A-k1v*V*H1*A
H2A'=k2s*S*H2*A+k2v*V*H2*A
H2'=-k2s*S*H2*A-k2v*V*H2*A
A'=-k1s*S*H1*A-k1v*V*H1*A-k2s*S*H2*A-k2v*V*H2*A
//
H1TOT=H1+H1A
H2TOT=H2+H2A
ATOT=A+H1A+H2A
//
T=0
V=V0
S=S0
ATP=ATP0
```

H1A=H1A0
H1=H10
H2A=H2A0
H2=H20
A=A0
***
The following abbreviations are used

Dependent variables: H1A = **2A**; H2A = **1A**; V = vesicle; S = surfactant; ATP = **ATP**; H1 = **2**; H2 = **1**; A = **A**;

Parameters:

indicator		
ka	association rate constant vesicle assembly	1.00E+10
kd	dissociation rate constant vesicle disassembly	1.00E+00
kcat	rate constant for ATP hydrolysis	1.50E+04
k1s	rate of formation for H1A in non-assembled state	4.99E+04
k1v	rate of formation for H1A in assembled state	3.21E+04
k2s	rate of formation for H2A in non-assembled state	9.09E+03
k2v	rate of formation for H2A in assembled state	7.29E+04
V0	Initial vesicle concentration	Simulation dependent
S0	Initial surfactant concentration	Simulation dependent
ATP0	Initial ATP concentration	Simulation dependent
H1A0	Initial concentration of H1A	Simulation dependent
H2A0	Initial concentration of H2A	Simulation dependent
H10	Initial concentration of H1	Simulation dependent
H20	Initial concentration of H2	Simulation dependent
A0	Initial concentration of A	Simulation dependent

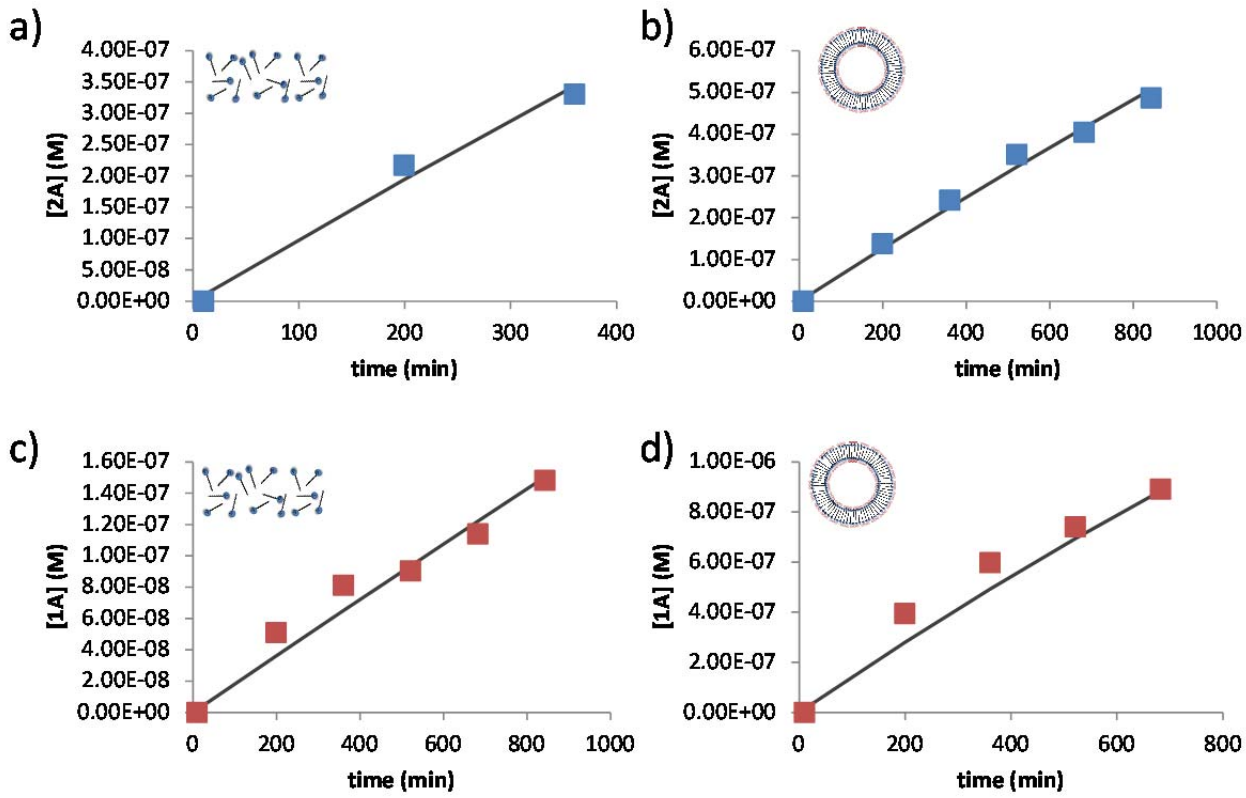

Figure S29. Fits of the data reported in Figure 3b and d to the kinetic model to obtain the values for k1s (a), k1v (b), k2s (c) and k2v (d) reported above.

6. References

1. Fulmer, G. R.; Miller, A. J. M.; Sherden, N. H.; Gottlieb, H. E.; Nudelman, A.; Stoltz, B. M.; Bercaw, J. E.; Goldberg, K. I. *Organometallics***2010**, *29*, 2176.
2. Maiti, S.; Fortunati, I.; Ferrante, C.; Scrimin, P.; Prins, L. J. *Nat. Chem.***2016**, 8, 725.
3. Gasparini, G.; Martin, M.; Prins, L. J.; Scrimin, P. *Chem. Commun.***2007**, 1340.